J. Fluid Mech. (1970), *vol.* 42, *part* 2, *pp.* 295–307
Printed in Great Britain

On the transition to turbulent convection. Part 1. The transition from two- to three-dimensional flow

By RUBY KRISHNAMURTI
Geophysical Fluid Dynamics Institute, Florida State University

(Received 7 July 1969)

In a horizontal convecting layer several distinct transitions occur before the flow becomes turbulent. These are studied experimentally for several Prandtl numbers from 1 to 10^4. Cell size, plan form, transitions in plan form, transition to time-dependence, as well as the heat flux, are measured for Rayleigh numbers from 10^3 to 10^5. The second transition, occurring at around 12 times the critical Rayleigh number, is one from steady two-dimensional rolls to a steady regular cellular pattern. There is associated with this a discrete change of slope of the heat flux curve, coinciding with the second transition observed by Malkus. Transitions to time-dependence will be discussed in part 2.

Introduction

The transition to turbulence was understood by Malkus (1954*b*), and by Landau (Landau & Lifshitz 1959) to occur in the following manner: at sufficiently low values of the determining parameter the flow is stable to all disturbances. As the value of the parameter is increased the flow becomes unstable to more and more kinds of disturbances. At sufficiently large values of the parameter, the flow is unstable to so many kinds of disturbances, each occurring with random phase, that it is difficult to describe and is unpredictable in detail. The flow is then called turbulent. Unlike the fast transition to turbulence in pipe and channel flow, the flow in a horizontal convecting layer undergoes a number of discrete transitions, remaining in each régime for a finite range of Rayleigh number, which is the determining parameter in this problem.

This paper, and a following one, are reports on experimental studies of transitions in a horizontal layer of fluid which is heated uniformly from below and cooled uniformly from above. There are two† dimensionless parameters describing this problem. They are the Rayleigh number R, and the Prandtl number Pr, defined as follows:

$$R = (g\alpha/\kappa\nu)\,\Delta T d^3, \quad Pr = \nu/\kappa,$$

where g is the acceleration of gravity, α the thermal expansion coefficient, κ the thermal diffusivity, ν the kinematic viscosity, d the layer depth, ΔT the temperature difference across the layer. In the order of increasing R, the first transition

† The third dimensionless parameter, which may be taken to be the aspect ratio (the ratio of depth to horizontal extent of the layer), is made small in all these experiments in an attempt to approximate a horizontally infinite layer. Effects of varying this aspect ratio are discussed later.

occurs at the well-known critical Rayleigh number R_c, which is independent of Prandtl number. This transition is from the conduction state to a state of steady cellular convection. The nature of the flow and the change in slope of the heat flux curve have been predicted and experimentally verified. For the vertically symmetric problem the only stable finite amplitude solution of the infinite number of possible steady solutions is the two-dimensional roll (Schlüter, Lortz & Busse 1965). With a vertical asymmetry, such as that produced by changing mean temperature or by variation of material properties (ν, κ, α) with temperature, the conduction state is subcritically unstable to finite amplitude disturbance, and the flow near the critical point is hexagonal (Busse 1962; Segel & Stuart 1962; Krishnamurti 1968*a*, *b*). In this paper we restrict our attention to the case in which rolls are the realized flow just above R_c.

Higher transitions in the heat-flux curve were observed by Malkus (1954*a*) and confirmed by Willis & Deardorff (1967). It was pointed out by Malkus that these transitions occur at Rayleigh numbers corresponding to the linearly predicted instability point for the onset of higher vertical modes. However, it is difficult to understand how an instability predicted on a linear conduction profile can have such a distinct effect in changing the slope of the heat-flux curve at Rayleigh numbers where the state is no longer one of conduction. In none of the previous studies was there an attempt to observe whether or not a change in the flow pattern accompanies these distinct changes in slope. One observational study by Rossby (1966) shows that for Prandtl number 10^2, rolls are replaced by three-dimensional flow at Rayleigh number between $6R_c$ and $15R_c$. However, it is not known if there was a concomitant change of slope of the heat-flux curve.

The only theoretical study of stability of two-dimensional convection in this Rayleigh number range is that of Busse (1968). He shows that for infinite Prandtl number, two-dimensional rolls having wave-number β within a finite band (see figure 13) are stable to a restricted class of infinitesimal disturbances provided that $R < 22{,}600$. If $R > 22{,}600$ rolls are unstable for all β. Busse shows further that the roll plan form is then unstable to a disturbance of rectangular form with one side along the original roll axis. It is not known from this theory whether the resulting flow above 22,600 is steady. It is also not known how the selection of β from this band of possible wave-numbers occurs either in an infinite plane or in an experiment approximating an infinite horizontal layer. (This approximation is in the sense of Segel (1969), who shows that, for aspect ratio sufficiently small and for straight rather than curved rolls, only the edge rolls are affected by the side walls.)

The following questions become conspicuous. In what region of the space of the parameters (R, Pr) does one observe steady two-dimensional rolls? What is the nature of the three-dimensional flows? Are there regions of parameter space where they are regular in spacing, steady in time? Are there time-dependent two-dimensional flows? Are these transitions related to Malkus's discrete changes of slope of the heat flux curve? We attempt to answer some of these questions.

The study was conducted as a series of externally steady, fixed heat-flux experiments. As such, it is free from the criticism, as expressed by Elder (1965) for example, of Malkus's experiments, which were quasi-steady. The experiments

of Willis & Deardorff were also quasi-steady. The cell size, the plan form, and transitions in plan form, as well as the heat flux and the temperature-difference across the layer were measured for several fluids with Prandtl numbers in the range 10–10^4. The steadiness or time-dependence of the flow was tested by the technique described in part 2. All experiments reported here in part 1 were found to be time-dependent.

Apparatus and procedure

The experimental apparatus is shown schematically in figure 1. The fluid layer occupies a region 51 by 49 cm, with a variable depth of 0·498, 0·988, 1·984, 3·007, or 5·000 cm. The plexiglass tank containing the fluid also contains four blocks of aluminium 6061 T 651. Two of the blocks are 4 in. thick, two are 1 in. thick, each is 20 in. by 20 in. wide. The electrical heater, which is a fine mesh of resistance material embedded in silicon rubber, is attached to the bottom of the lowest block, which is 4 in. thick. The heater is further protected by an additional plate of $\frac{1}{4}$ in. thick aluminium bolted on to the block and by sealing compound which isolate the heater from the fluid. The heat input is controlled by a variable transformer backed by a constant voltage transformer of the line voltage. Above this lowest aluminium block is a low-conductivity layer of methyl methacrylate. A layer of liquid sufficiently thin that it never convects for the temperature gradients occurring in these experiments effects constant thermal contact between the layers. Above this low conductivity layer is a block of aluminium 1 in. thick; above this is the convecting fluid, whose depth is defined by plexiglass spacers. The arrangement of blocks above the convecting layer is symmetric to that below except that the cooling is accomplished by cooling fluid from a constant-temperature circulator flowing in channels in the uppermost aluminium block. The channels for incoming and outgoing flows are side by side in order to minimize horizontal temperature gradients. The channels were cut in a complicated pattern and spaced so that the separation of channels was not close to an integral multiple of the expected convection cell size. The maximum flow rate of the cooling fluid is 2·5 gal/min.

The thermal diffusivity of the aluminium blocks is 0·87 cm^2/sec, which is about three orders of magnitude larger than that of most liquids. This is, of course, an attempt to approach the ideal condition of perfectly conducting boundaries. With poorly conducting boundaries a horizontal temperature ripple corresponding to the cellular structure in the convecting fluid penetrates into the boundaries and may control transitions to different cellular structures. Also the aluminium acts as a diffuser of any horizontal temperature variations arising from the discrete nature of the cooling channels. The large mass of metal of approximately 400 lb. acts as a large heat capacity so that temperatures in the blocks are very stable. The blocks were lowered into place with the aid of a chain hoist. The aluminium plates bounding the fluid were levelled to $\pm$ 0·0003 in. in 12 in.

The above is a description of apparatus presently in use at F.S.U. Apparatus of similar construction was used earlier at Stanford University and another was used still earlier at U.C.L.A. The latter, however, contained a fluid layer which

was 30 by 30 cm in horizontal extent. Also, since it was originally designed for another experiment, it did not have a constant-temperature cooling bath. The cold temperature was maintained by adding ice to a reservoir at regular intervals (once every $\frac{1}{2}$h for as long as 36 h).

To determine the heat flux and the temperature difference across the fluid layer, four pairs of copper-constantan thermocouples were used. These were made using 'thermal free' solder and pure resin in alcohol flux to prevent the occurrence of

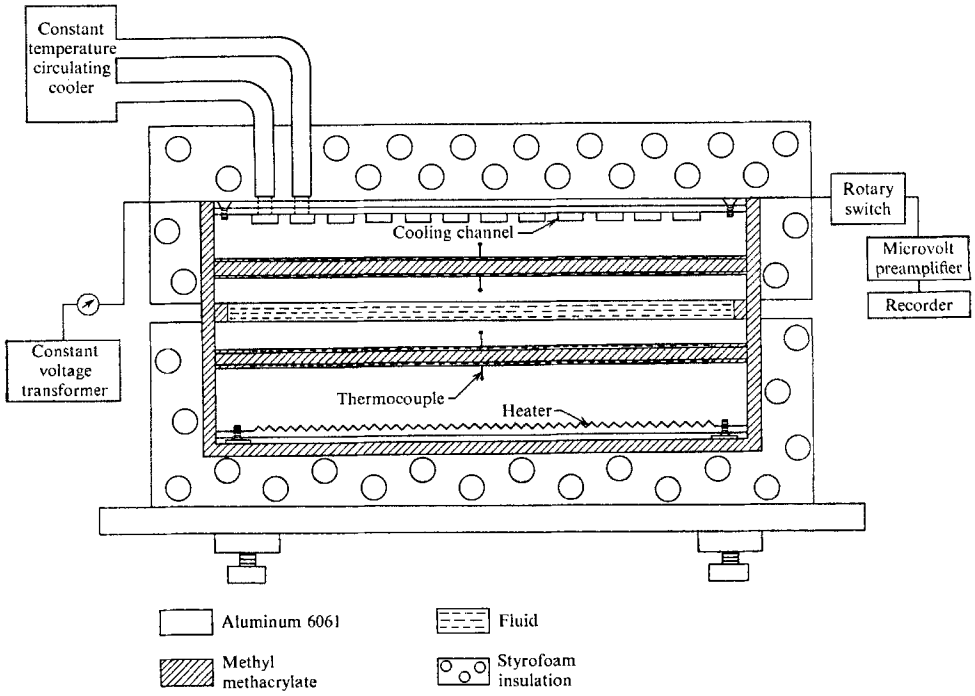

FIGURE 1. A schematic diagram of the apparatus for studying horizontal convection.

extraneous emf's. After calibrating them, care was taken not to stress them excessively. One junction was embedded in each of the aluminium blocks, but was electrically isolated from it. The remaining four junctions were placed in a common constant-temperature bath. Since the aluminium has high conductivity, vertical temperature gradients within it are small (of the order of 10^{-3} °C/cm), horizontal gradients are even smaller, so that the positioning of the thermocouples within the blocks is not crucial. By means of a rotary switch the emf's from each of the thermocouple pairs were sampled in turn (approximately once every minute). The signals were amplified on a Keithley microvolt amplifier whose accuracy is ± 2 % of full scale on all ranges. It has 14 overlapping ranges from 0·3 μV full scale to 1 V full scale. Most of the signals encountered in this part of the study were of the order of 10–100 μV. The zero drift is less than 0·1 μV in 24 h, and long-term drift is not cumulative. The input noise is less than 5 nV rms on the most sensitive range. The Keithley recorder is matched to the amplifier.

The heat transported by the convecting liquid is measured by concentrating

the temperature gradient across the poor conductor in the manner devised by Malkus (1954*a*). In the steady state the heat H transported by the fluid is the average of the heat conducted across the two poor conductors:

$$H = k_p \frac{T_1 - T_2}{2d_p} + k_p' \frac{T_3 - T_4}{2d_p},$$

where k_p and k_p' are the molecular conductivities of the low conductivity layers, d_p is the depth of the layer, and T_1, T_2, T_3 and T_4 are the temperatures of the four aluminium blocks. The subscripts are ordered from bottom to top. The conductivities k_p and k_p' are measured in terms of that of the liquid when it is known that the liquid layer is in a state of steady conduction. Then the following relations hold:

$$k_f \frac{T_2 - T_3}{d} = k_p \frac{T_1 - T_2}{d_p} = k_p' \frac{T_3 - T_4}{d_p},$$

where k_f is the molecular conductivity of the fluid.

Had the heat flux been measured by the electrical power input, correction must be made for the major heat loss downward. The present method is independent of the heat lost by block 1 and gained by block 4. The loss and gain by the blocks 2 and 3 are determined as follows:

$$k_p \frac{T_1 - T_2}{d_p} = Q + q, \quad k_p' \frac{T_3 - T_4}{d_p} = Q + q,$$

where Q is the heat flux through the liquid layer, q the flux through the side walls (out at block 2, in at block 3; $H = Q + q$). Since the heating and cooling is symmetric about room temperature,

$$\frac{q}{Q} = \frac{a}{A} \left(\frac{k_p(\Delta T/2l)}{k_f(\Delta T/d)} \right),$$

where A is the horizontal area of the liquid layer, a the vertical area of the side walls surrounding blocks 2 and 3, and l is the thickness of the side wall. This ratio is about 0·05 in the conduction régime, and even smaller in the convection régime.

Fine aluminium flakes suspended in the liquid were used to visualize the flow. A sufficiently small quantity was added so that the visibility through 20 in. of the liquid was not impaired. The aluminium flakes become aligned in a shear flow, and because they are flakes, reflect light more strongly in certain directions, depending upon the direction of the shear and of the illumination. In a uniform shear, the brightness is uniform; where there is a differential shear, there will be corresponding bright and dark regions. In the case of water, aluminium flakes would not stay in suspension sufficiently long, so another tracer called 'rheoscopic fluid† AQW 010' was added to the water. This tracer displays differential shears, just as do the aluminium flakes, but remains in suspension about 10 times as long.

Since the fluid layer is bounded above and below by opaque boundaries, the plan form of convection is obtained by viewing the flow from the side as previously described (Krishnamurti 1968*b*). The tracers were illuminated at mid-depth by narrow overlapping beams of collimated light from two 2 W zirconium

† Made by Kalliroscope Corporation, Cambridge, Massachusetts.

arc lamps. The light source is 0·005 in. in diameter and of very high surface brightness. The diameter of the beam through the fluid was 2–3 mm. The two beams directed at each other allow visualization of shear regions at both positive and negative angles to the line of sight. This line of sight is perpendicular to the beam. As the light beam is moved horizontally, illuminating different regions of the fluid, a camera is moved horizontally on a threaded rod in order to keep the illuminated region in focus. Simultaneously, the back of the camera rolls on an inclined plane since the camera is free to rotate about an axis through its lens. Thus, different regions of the fluid produce images on different parts of the film.

Fluid	Prandtl number (Pr)	Kinematic viscosity (centistokes) at 25 °C	Thermal diffusivity (cm^2/sec)	Thermal expansion coefficient ($°C^{-1}$)	Layer depth d (cm)
Air	0·71	18·5	0·264	$3·37 \times 10^{-3}$	5
Water	6·7	1·00	$1·43 \times 10^{-3}$	$2·13 \times 10^{-4}$	1, 2, 3
Dow Corning '200' silicone oil	57	5·0	$0·88 \times 10^{-3}$	$1·05 \times 10^{-3}$	1, 2, 3
Dow Corning '200' silicone oil	102	10·0	$0·98 \times 10^{-3}$	$1·08 \times 10^{-3}$	2, 3
Chevron white oil no. 1	210	15 (at 24 °C)	$0·71 \times 10^{-3}$	10^{-3}	2
Dow Corning '200' silicone oil	860	100	$1·16 \times 10^{-3}$	$0·96 \times 10^{-3}$	3
Dow Corning '200' silicone oil	8500	1000	$1·18 \times 10^{-3}$	$0·96 \times 10^{-3}$	5

TABLE 1

In this way, one obtains a picture of the flow pattern as if one were viewing from above. The necessary hardware for the photography (synchronous motor, gears, threaded rods, power supplies, microswitches, etc.) was mounted on a rigid frame built around the convection tank. The entire apparatus was enclosed in a light-tight house.

The routine for obtaining the data was as follows: the fluid was stirred while in an isothermal state, to produce a uniform distribution of tracer. The input voltage to the heating element was fixed at some desired value by setting the variable transformer. The temperature of the cooling fluid was adjusted until all four aluminium blocks reached a steady temperature. Since the resistance of the heating element is then steady, the power input to the system is steady. The four temperatures were recorded and a photograph of the plan form was obtained. The photography was repeated until the flow pattern showed no further changes. Then the heat input was changed by a few per cent and the process repeated.

At first it was tacitly assumed that the discrete changes of slope of the heat-flux curve could be observed only in a passive system, such as a slowly decaying situation, which produces data points with negligible scatter. Thus, the fixed heat-flux data was obtained in no particular order. However, when this data was plotted against Rayleigh number two straight lines could be distinguished with

considerable scatter near the transition points. This interpretation became even clearer when the data points were separated according to the past history of the system (whether the previous state was one of higher or lower Rayleigh number and how rapidly the state had been attained). Thus, the experiments were repeated, obtaining data at closer intervals of Rayleigh number, and in the following order: starting at some low value of H and R, H was increased by a few per cent, the data recorded after steady state was attained, then H was increased again by a few per cent. At no time was it allowed to decrease until a desired upper value of H, R was attained. The system was then taken to a low value of (H, R) by small decreases in H, separated by steady states. Thus the system was continuously convecting for periods of several weeks.

Care was taken to perform all experiments symmetrically, heating and cooling by the same amount about room temperature. Non-Boussinesq effects were kept below 2 % by using temperature differences less than about 2 °C.

The procedure was repeated for the fluids (except air) whose properties are listed in table 1.

Experimental results

A typical plot of heat flux H *versus* Rayleigh number R is shown in figure 2. H has been non-dimensionalized so that the conductive heat flux equals R; that is, $H = NR$ where N is the Nusselt number. The data is very well represented by two intersecting straight lines. The transition Rayleigh number R_{II}, at which there is a change of slope when R_{II} is approached from below, is listed in table 2. The other fluids displayed the same distinct change of slope as seen in figure 2, but there was an unexplained difference in the magnitude of this change of slope. The relevant data is shown in table 2. The value of R_{II} for $Pr = 6{\cdot}7$ coincides with the second transition observed by Malkus (1954*a*), in one case, in water.

The scatter in the data as seen in figure 2 is of the order of the amplifier sensitivity, which is also approximately the error in reading the instrument. The error in determining R_{II} is about ± 15 % in this case. In cases in which all the data was not obtained in one continuous run, the error in determining R_{II} is larger.

The values of R_{II} for the various fluids are not interpreted as showing a definite Prandtl-number dependence since the transition is one displaying hysteresis. When R_{II} is approached from above, the heat flux is larger than that obtained when R_{II} is approached from below. This is seen in figure 3. Also, the three-dimensionality (discussed below) persists below R_{II}. It is suggested that the two heat-flux states are metastable states above some finite Rayleigh number (about $4R_c$). The lower-heat flux state, with two-dimensional flow, is attained if the Rayleigh number is increased in small steps from below. If a Rayleigh number R such that $4R_c < R < R_{\mathrm{II}}$ is attained from below and the fluid is then stirred, the resulting state was found to be on the upper heat flux curve.

The additional transition observed by Willis & Deardorff at $4{\cdot}8R_c$ is not apparent in figure 4, where the range and steps of R were chosen to look for this transition. The above discussion helps clarify this discrepancy. Three-dimensional flows have been observed at about $5R_c$ by Koschmieder (1966), by

Krishnamurti (1967) due to sudden change in R (see figure 8), and in the present study with Rayleigh number decreased from above R_{II}. The hysteresis found in the present study implies a finite ampitude instability which may be excited below R_{II} by a number of disturbances which would be difficult to trace.

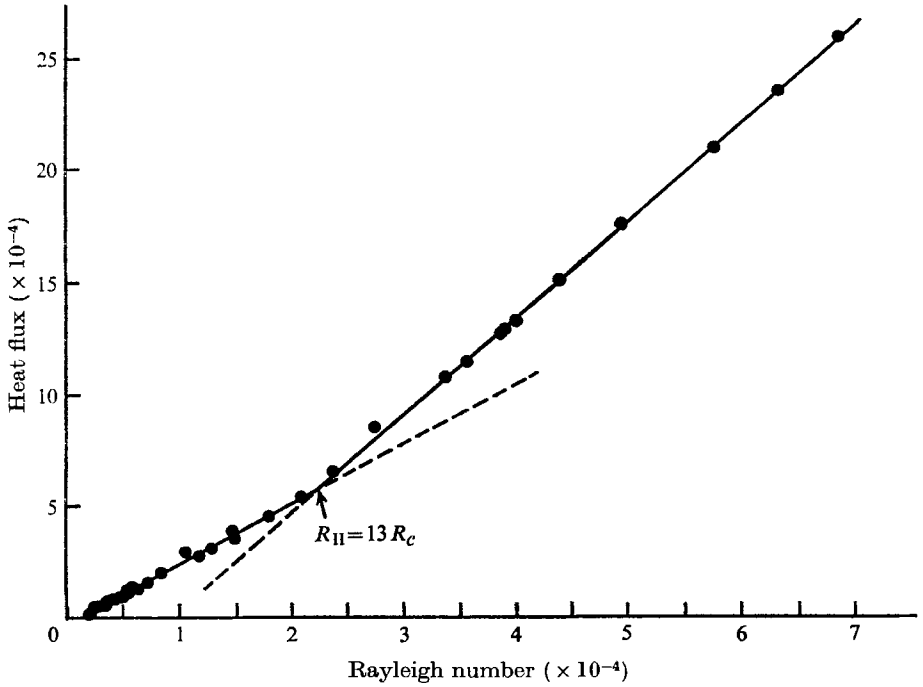

FIGURE 2. Heat flux plotted against Rayleigh number, showing the second transition. The heat flux has been non-dimensionalized so that it is the product of Nusselt and Rayleigh numbers. The Prandtl number is $1{\cdot}0 \times 10^2$.

Pr	d(cm)	R_{II}	Slope $\frac{dH}{dR}$ for $R < R_{II}$	Slope $\frac{dH}{dR}$ for $R > R_{II}$	Change of slope
6·7	1	—	$2{\cdot}7_2$	—	—
6·7	2	$10R_c \pm 6\%$	$2{\cdot}7_7$	$4{\cdot}6_6$	1·9
57·0	2	$13R_c$	—	—	—
100·0	2	$13R_c \pm 15\%$	3·0	4·3	1·3
860·0	3	$13R_c \pm 25\%$	3·1	4·1	1·0
8500·0	5	$10R_c \pm 5\%$	3·4	4·2	0·8
$Pr \to \infty$	—	$13R_c$†	—	—	—

† This is the value computed by Busse (1968).

TABLE 2. Transition Rayleigh number, R_{II}, for various Prandtl numbers, Pr

The change of slope at R_{II}, when R_{II} was approached from below, was accompanied by a change in plan form from two-dimensional to three-dimensional flow. Photographs of the plan form (obtained from the side of the tank) are shown in figures 5 to 8 (plates 1–3). These will now be described in detail.

To find the point at which two-dimensional rolls become unstable, giving rise to three-dimensional flow, one must clearly start with well-defined rolls. The evolution of the plan form to two-dimensionality at a fixed Rayleigh number below R_{II} is shown in figures 5(*a*, *b*) (plate 1). As explained previously (Krishnamurti 1968*b*), in a square container rolls start in a square array if the system is

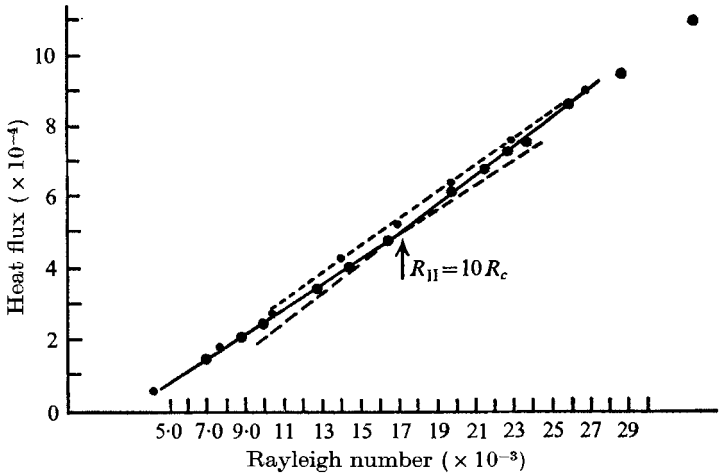

FIGURE 3. Heat flux plotted against Rayleigh number, showing hysteresis near the second transition. The Prandtl number is 0·85 × 10⁴. –●–●–●–, R increased; –●– – ●–, R decreased.

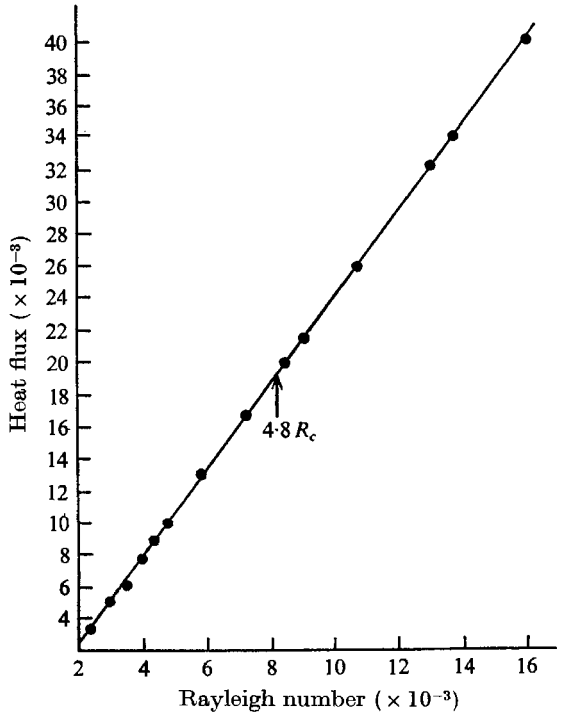

FIGURE 4. Heat flux plotted against Rayleigh number near $4·8R_c$. The Prandtl number is 6·7.

taken slowly through R_c, but never remain in this form. The time scale for rearrangement is understood as follows. The vertical thermal diffusion time $\tau_t = d^2/\kappa$ is of the order of hours ($\frac{1}{2}$–7 h in these experiments). The horizontal thermal diffusion time is 1 month for the 50 cm wide tank. The viscous diffusion time d^2/ν is of the order of seconds or minutes. Suppose that at sufficiently low Rayleigh number three-dimensional flow is unstable, but exists initially because of the geometry of the container. As the three-dimensionality decays, the neighbouring cells must adjust to the change. This adjustment can occur by information propogating by diffusion or by advection. Newell & Whitehead (1969) show that spatial non-uniformities of small but finite amplitude propagate by diffusion with time scale

$$\tau_d = \frac{Pr+1}{Pr}\frac{L^2}{\kappa} \tag{1}$$

to some characteristics distance L. For larger Pr this becomes the thermal diffusion time, for small Pr the viscous diffusion time. It is noted that for R near R_c the orbit time of a parcel of fluid,

$$\tau_0 \simeq \left(\frac{R_2}{R-R_c}\right)^{\frac{1}{2}}\frac{d^2}{\kappa}, \tag{2}$$

is much greater than the diffusion time τ_t. Here R_2 is a number dependent upon Pr, computed by Schlüter, Lortz & Busse to be of the order of R_c. For some larger R the orbit time becomes smaller than the diffusion time. The neighbouring cell then takes at least an orbit time (not necessarily given by (2) above) to readjust. After this time the next adjacent cell must readjust. Thus, the time required is the number N of cells across the container times τ_0, which depends upon Rayleigh number. The readjustment time is therefore greater than the vertical diffusion time but less than the horizontal diffusion time. The two tanks used had horizontal size $L_1 = 30$ cm and $L_2 = 50$ cm. Comparing cases in which d, κ and R had the same values in both experiments, so that N is proportional to L_1 in one case and to L_2 in the other, the ratio of the time for straightening of the rolls was L_1/L_2 rather than $(L_1/L_2)^2$. The resulting straight rolls are what Segel (1969) calls 'spatially modulated' rolls in a 'shallow dish'. For these the distortion due to the side walls disappears within the width of two rolls. After the rolls became straight, or nearly so, there was no further tendency to change. Figures 5(*b*) (plate 1), and 6(*a*) (plate 2) are examples of almost straight rolls which began as rolls in a square array. The difference in heat flux between the initial rolls in the square array and the final straight rolls is not more than the scatter shown in the heat flux curve in figure 2.

After the rolls became straight the heat flux, and hence the Rayleigh number, were increased in small steps punctuated by long periods of steady external conditions. It was found that the only change that occurred below R_{II} was an increase in the width of the roll. This is seen in figure 5(*c*) (plate 1). Figures 5(*c*) and 6(*c*) (plate 2) show a three-dimensional structure over part of the region which is not inconsistent with the concept of metastable states.

When R was increased to a value greater than R_{II}, a disturbance was seen to form on the rolls. In figures 5(*e*) (plate 1), 6(*b*, *d*) (plate 2) the flow is obviously

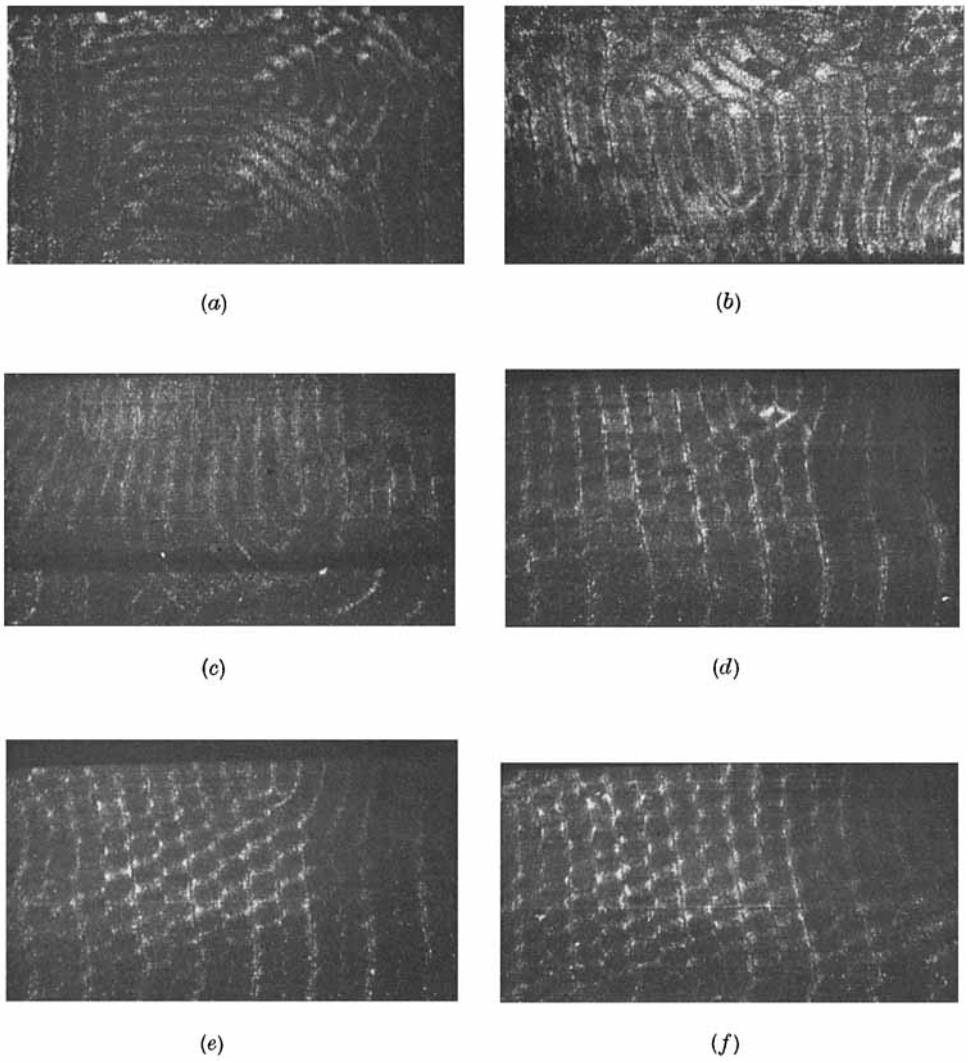

FIGURE 5. The plan form of convective flow, Prandtl number $1{\cdot}0 \times 10^2$. (*a*) $R = 3{\cdot}2R_c$, day 1; the flow pattern shows the influence of a square boundary. (*b*) $R = 3{\cdot}2R_c$, day 4, the flow pattern is approaching the form of straight rolls. (*c*) $R = 6{\cdot}8R_c$, day 6. (*d*) $R = 12{\cdot}1R_c$, day 8. (*e*) $R = 15R_c$, day 9. (*f*) $R = 20R_c$, day 10.

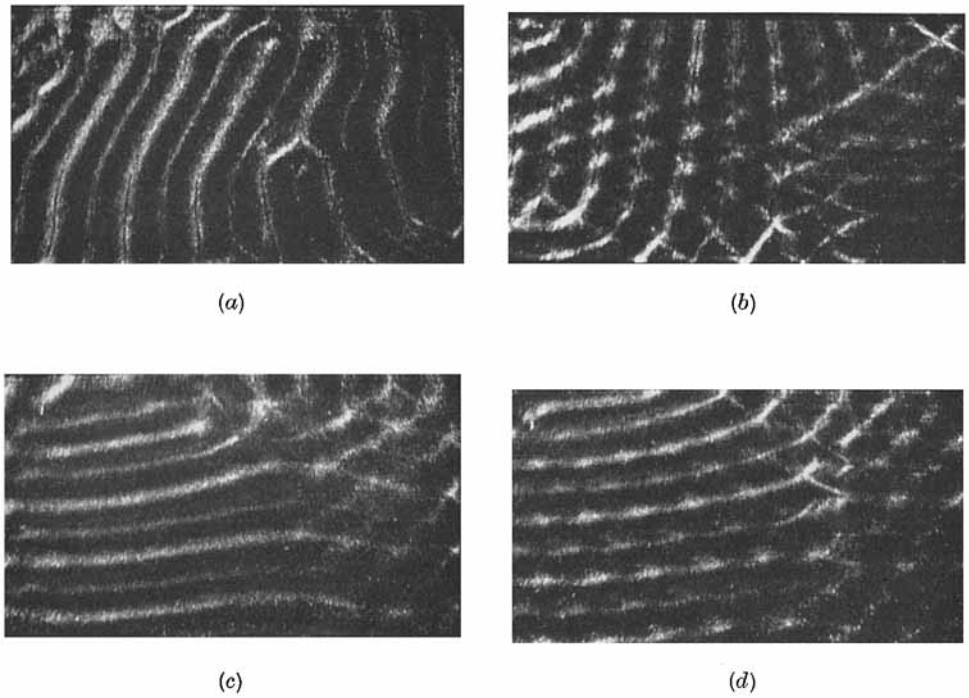

FIGURE 6. The plan form of convective flow, Prandtl number $0{\cdot}86 \times 10^3$. (*a*) Rolls parallel to one wall, $R = 2{\cdot}7\,R_c$ and (*b*) the three-dimensional disturbance that forms on these rolls, $R = 12\,R_c$. In a repetition of the same experiment, rolls perpendicular to those in (*a*) are seen in (*c*), $R = 9{\cdot}0\,R_c$ and (*d*) shows the three-dimensional disturbance that formed on the rolls seen in (*c*), $R = 12{\cdot}2\,R_c$.

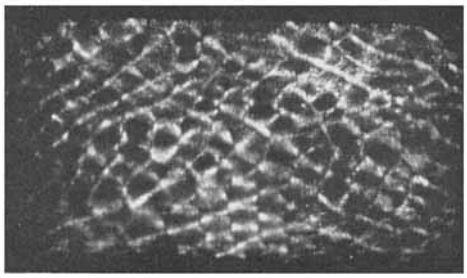

FIGURE 7. The plan form of convective flow, $R = 33R_c$, Prandtl number is 57.

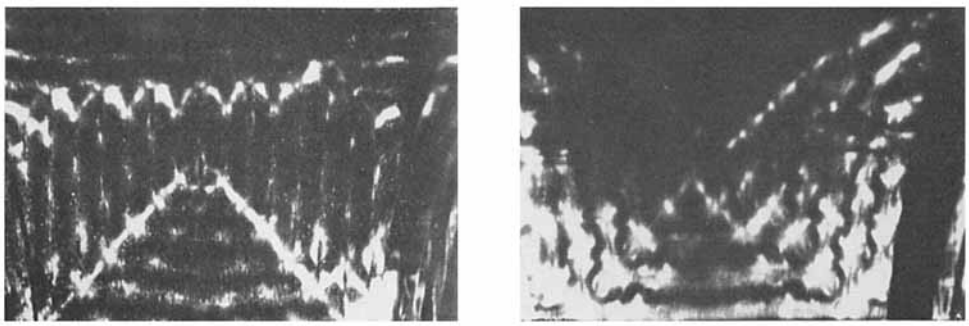

(*a*) (*b*)

FIGURE 8. Plan forms of convection for Prandtl number $1{\cdot}7 \times 10^3$. (*a*) $R = 1{\cdot}8R_c$, $dR/dt = 0$, (*b*) $R = 4R_c$, $1/R_c\, dR/dt = 6 \times 10^{-5}$ sec^{-1}.

three-dimensional. (Photographs of the plan form were obtained at frequent intervals, but only those showing a distinct change are shown here.) The change in flow pattern occurs at a Rayleigh number coinciding with R_{II}, within experimental error.

It was stated that the heat flux curve of figure 4 shows no change of slope at $4{\cdot}8R_c$. The flow pattern also showed no marked change up to about $10R_c$ except for an increase in roll width.

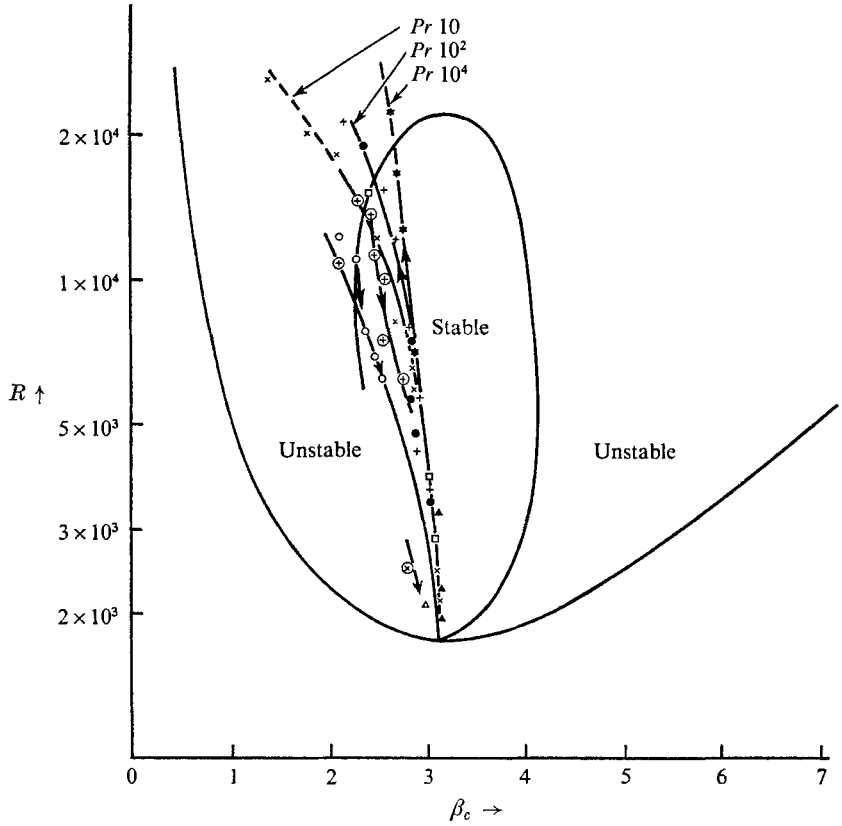

FIGURE 9. The observed cell size plotted on Busse's stability diagram for two-dimensional rolls.

	d (cm)	R increasing	R decreasing
Pr 6·7	1·2	×	⊗
Pr 57	2	□	
Pr 10^2	2	+	⊕
Pr $0{\cdot}86\times10^3$	3	●	○
Pr $1{\cdot}7\times10^3$	5	▲	△
Pr $0{\cdot}85\times10^4$	2	★	

Both Davis (1967) and Segel (1969) show that spatially modulated rolls will line up with their axes parallel to the short side of a rectangular container. In this experiment conducted in an almost square container, there appears to be little preference of orientation of the rolls. Figures 6(*a*, *c*) (plate 2) show rolls along the line of sight and perpendicular to the line of sight in two different repetitions of the same experiment.

The three-dimensional disturbance that forms on the rolls above R_{II} is consistent with Busse's instability to a rectangular disturbance. Since the method of photography displays regions of strong shear, the hypotenuse of the rectangle should appear bright. Thus, the nature of the growing mode (which is found experimentally to attain a steady state) is in agreement with Busse's result. It may be noted that the rectangular disturbance of his theory is one with symmetry in the vertical. The point of transition is also in good agreement with that computed by Busse, for that wave-number β which occurs in the experiment, although the selection mechanism of that β is not understood.

For R just above R_{II}, the original rolls are distinguishable and the rest of the flow pattern may be called a disturbance. As R is increased still further, the disturbance becomes more prominent. At $33R_c$ the flow pattern, as seen in figure 7 (plate 3), is entirely three dimensional.

When the Rayleigh number is decreased from a value above R_{II}, again in small steps punctuated by long periods (days) of steady state, the three-dimensionality remains to Rayleigh numbers smaller than R_{II}. For Prandtl number $0{\cdot}86 \times 10^3$ the three-dimensionality was apparent as low as $7R_c$, and for Prandtl number $0{\cdot}85 \times 10^4$, as low as $4{\cdot}5R_c$. The cell size is also larger than at the corresponding Rayleigh number approached from below.

The observed wave-number β (equal to π times the layer depth divided by the observed roll width) is plotted on Busse's stability diagram in figure 9. The arrows indicate whether R was increased from below or decreased from above. Hysteresis in β is apparent. Care was taken to measure only straight rolls so that one unambiguous number could be obtained. The broken lines in figure 9 represent the observed wave-number after a three-dimensional disturbance has set in. In this case β refers to the wave-number of the rolls (which are still distinguishable). It is seen from figure 9 that the cell size depends upon Prandtl number, perhaps upon aspect ratio, and most definitely upon its past history. Most notable is the fact that, when the cell size is allowed to evolve freely (without being forced as in the experiments of Chen & Whitehead 1968), approximately one-half of Busse's stability diagram is filled with observations, but the domain $\beta > \beta_c$ is conspicuously bare.

Conclusions

There is a second transition in a horizontal convecting layer, characterized by the following properties:

(i) There is a discrete change of slope of the heat flux curve at Rayleigh number R_{II} near $12R_c$, showing no definite Prandtl number dependence in the range $10 < Pr < 10^4$.

(ii) There is a change in the flow pattern from two-dimensional rolls to a three-dimensional flow which is periodic in space and steady in time. The change occurs at a Rayleigh number coinciding with R_{II} to within the error in determining R_{II}.

(iii) There is hysteresis in the heat flux as well as in the flow pattern as R is increased from below or decreased from above, indicating that the transition is caused by a finite amplitude instability.

The paper is also part of Geophysical Fluid Dynamics Institute, Florida State University, Contribution 24. The research was supported at UCLA under grant GP-2414 of the National Science Foundation, at Stanford University under a grant from the Office of Saline Water, and at the Florida State University under Office of Naval Research Contract N 00014-68-A-0159, where the largest part of the work was done. I am grateful to Professor W. V. R. Malkus, to Professor Andreas Acrivos, and to Professor Richard L. Pfeffer for this support.

REFERENCES

BUSSE, F. H. 1962 Dissertation, University of Munich. (Translation from the German by S. H. Davis, the Rand Corporation, Santa Monica, California, 1966.)

BUSSE, F. H. 1968 *J. Math. Phys.* **46**, 140.

CHEN, M. M. & WHITEHEAD, J. A. 1968 *J. Fluid Mech.* **31**, 1.

DAVIS, S. H. 1967 *J. Fluid Mech.* **30**, 465.

ELDER, J. W. 1965 *J. Fluid Mech.* **23**, 77.

KOSCHMIEDER, L. 1966 *Beit. Z. Phys. Atmos.* **39**, 1.

KRISHNAMURTI, R. 1967 Dissertation, University of California at Los Angeles.

KRISHNAMURTI, R. 1968*a* J. *Fluid Mech.* **33**, 445.

KRISHNAMURTI, R. 1968*b* *J. Fluid Mech.* **33**, 457.

LANDAU, L. D. & LIFSHITZ, E. M. 1959 *Fluid Mechanics*. Oxford: Pergamon.

MALKUS, W. V. R. 1954*a* *Proc. Roy. Soc.* A **225**, 185.

MALKUS, W. V. R. 1954*b* *Proc. Roy. Soc.* A **225**, 196.

NEWELL, A. C. & WHITEHEAD, J. A. 1969 *J. Fluid Mech.* **38**, 279.

ROSSBY, H. T. 1966 Dissertation, M.I.T.

SCHLÜTER, A., LORTZ, A. & BUSSE, F. 1965 *J. Fluid Mech.* **23**, 129.

SEGEL, L. A. 1969 *J. Fluid Mech.* **38**, 203.

SEGEL, L. A. & STUART, J. T. 1962 *J. Fluid Mech.* **13**, 289.

WILLIS, G. E. & DEARDORFF, J. W. 1967 *Phys. Fluids*, **10**, 1861.